Int. J. Solids Structures, 1969, Vol. 5, pp. 1171 to 1193. Pergamon Press. Printed in Great Britain

THE PERMANENT DEFORMATION OF A PORTAL FRAME SUBJECTED TO A TRANSVERSE IMPULSE†

G. L. JOHNSON‡

University of Hawaii

and

J. B. MARTIN§

Brown University

Abstract—A study is made of the inelastic response of a rectangular portal frame with a mass attached to the center of the beam to an impulse load transverse to the plane of the frame. The material is considered to be rigid–plastic, and the interaction between bending and torsion is considered on the basis of a rectangular yield curve. The ratio of the frame mass to the attached mass γ and the ratio of limit torsion moment to limit bending moment β are considered as variables. A simple two degree of freedom solution to a different initial value problem is presented which can be used to approximate the original problem in a rational manner. A comparison with an exact rigid–plastic solution is given for a limited range of values of β and γ. Experiments were carried out on steel and aluminum frames. The impulsive load was obtained by detonating blasting caps against the attached mass. The experiments showed evidence of the effects of the dependence of yield stress on strain-rate. When the rate sensitivity is included in the two degree of freedom solution in an approximate manner, good correlation between theory and experiment is obtained.

1. INTRODUCTION

THE inelastic response of ductile metal structures to dynamic loading is non-linear and presents severe analytical difficulties. The effects of strain-hardening, strain-rate sensitivity, elastic behavior and geometry changes compound the complexity of the analysis. Closed form solutions have been found for relatively few problems in this class. Although powerful numerical procedures have been developed (see, for example Witmer *et al.* [1]), there remains a need to seek analytical solutions to dynamic problems in order to provide a better physical understanding of the nature of the problem and to determine the most significant factors contributing to the response.

At the present time, the problem must be highly idealized if an analytical approach is expected to be successful. One of the most useful sets of idealizations introduced in recent years is that of the "elementary rigid–plastic theory" applied in particular to impulsive loading problems. In this theory it is assumed that the elastic contributions are insignificant, that the yield stress is constant and not affected by strain or strain rate. Geometry changes are neglected. In order for these assumptions to be valid, the magnitude of the dynamic

† The research reported in this paper was supported primarily by the Underwater Explosions Research Division, David Taylor Model Basin under Contracts N189(181)-59217A(X) and N189(181)-60723A(X). The experimental work was supported by the National Science Foundation under Grant GK1013.

‡ Assistant Professor, Department of Mechanical Engineering.

§ Professor of Engineering.

disturbance must be large enough that elastic effects are indeed negligible. Despite the apparent contradiction in that it is also assumed that geometry changes are small, this theory is applicable in many structural problems.

Early studies showed that particularly simple solutions could be obtained to certain problems on the basis of these assumptions (e.g. Lee and Symonds [2], Conroy [3], Hopkins and Prager [4], Symonds [5], Parkes [6]). Comparison of the theoretical predictions and experimental results have shown that while the assumptions of the elementary rigid–plastic theory lead to reasonable results, it is necessary to include strain hardening, rate sensitivity and geometry change effects in most cases to obtain good correlation. If attention is confined to structures in which geometry changes cannot contribute significantly, and to ductile metals in which very little strain hardening occurs, the discrepancy between the elementary theory and experiment must be caused by strain rate sensitivity, i.e. the dependence of yield stress on strain rate.

Parkes [6], in performing tests on cantilevers with an impulse at the tip, attempted to account for rate effects by using the elementary rigid plastic theory with an elevated yield stress based on an estimated average strain rate. The data of Manjoine [7] for the yield stress of mild steel as a function of strain rate was used. Bodner and Symonds [8] performed further tests on cantilevers, showing that better agreement could be obtained if a rate sensitive constitutive relation was used. Bodner and Symonds presented an approximate rate sensitive or rigid–visco-plastic analysis, and Ting [9] developed a more exact numerical procedure. The rigid–visco-plastic analysis is again extremely complex, but good agreement was obtained.

Some attention has been given to approximate methods of including rate sensitivity. Perrone [10] showed that good predictions of the final deformations could be obtained if the yield stress associated with the initial value of the strain rate in impulsively loaded simple structural elements is used.

Additional studies using the elementary rigid–plastic theory showed that early optimism regarding the simplicity of the theory was unfounded. Some simple structures, apparently suitable for the elementary rigid–plastic theory, proved extremely tedious to analyze and it became necessary to resort to numerical integration during part of the motion (e.g. Ezra [11], Gangopadhyay [12]). Recognizing that the simplicity of the rigid–plastic theory was one of its chief virtues, Martin and Symonds [13] developed a rational method of obtaining approximate elementary rigid–plastic solutions for impulsively loaded structures. The approximate solutions discussed by Martin and Symonds were mode solutions with one degree of freedom. They were extremely simple to obtain, and gave good results in many problems where a complete analysis was difficult.

Symonds [14] used the mode approximation technique as a starting point for an approximate theory including strain hardening and strain rate effects, and showed that adequate agreement with experiments could be obtained. Bodner [15] performed additional tests on cantilevers, and showed that an approximate visco-plastic theory based on the mode approximation and on Perrone's observations [10] gave good agreement.

Apart from simple beams, very few structures composed of straight bars have been studied. This class of structures has many advantages as an object of study, since they are used fairly widely in engineering practice and are nevertheless sufficiently simple that both analysis and experiments are fairly simple to carry out and to compare. It is the purpose of this paper to extend the idea discussed above to cover a structure in which two generalized stresses are important. The structure is shown in Fig. 1. A square portal frame has a mass

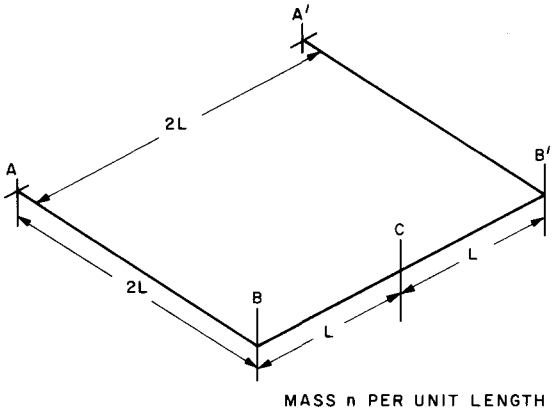

FIG. 1. Rectangular portal frame.

attached at the center of the beam, and the mass is subjected to an impulse in a direction transverse to the plane of the frame. Additional analytical difficulties are introduced because the interaction between bending and torsion must be included (shear deformation is neglected). The ratio of limit torsion moment to limit bending moment β and the ratio of the mass of the uniform frame to the attached mass γ are considered as variable parameters.

The analysis is carried out in an approximate manner, on the basis of elementary rigid–plastic theory. Comparison is made with the exact rigid–plastic analysis given by Johnson [16]. Visco-plastic effects are included in a manner similar to that suggested by Perrone [10], Symonds [14] and Bodner [15], and experimental results are presented which confirm the predictions within a limited range of values of the governing parameters.

The exact elementary rigid–plastic analysis of the problem was attempted by Johnson [16] on the basis of a simple idealized interaction between bending and torsion. This analysis is complex during the early stages of motion and the analysis is carried out only for limited regions in the β, γ domain. The mode approximation proves in this case to be inadequate for describing the motion, largely because it predicts that there will be no deformation of the beam to which the mass is attached. Thus, in this paper, an improved but nevertheless simple, approximation is presented. This approximation is based on the same arguments as those given by Martin and Symonds [13], and is valid over the entire range of values of β and γ. It is also shown that an approximate visco-plastic analysis may be constructed following the approach of Symonds [14] and Bodner [15], and a short series of experimental results is presented.

2. APPROXIMATE SOLUTIONS

Recently Martin and Symonds [13] have shown that a rational approximation for impulsively loaded rigid–plastic problems may be found using an argument similar to that required to prove uniqueness for this class of problems. The approximation has been shown to provide good estimates of the final deformation of the structure while eliminating the tedious and time consuming exact analysis of travelling hinge phases.

Suppose that, for a given structure two independent initial velocity fields v_i, v_i^* resulting from impulsive loading lead to responses characterized by velocities $\dot{u}_i, \dot{u}_i^*$, generalized stresses Q_j, Q_j^* and generalized strain rates $\dot{q}_j, \dot{q}_j^*$. No forces do work on the structure during the response. By the principle of virtual velocities

$$\int_s n(\ddot{u}_i - \ddot{u}_i^*)(\dot{u}_i - \dot{u}_i^*)\,\mathrm{d}s = \int_s (Q_j - Q_j^*)(\dot{q}_j - \dot{q}_j^*)\,\mathrm{d}s \tag{1}$$

where n is the mass per unit length, and the integration is carried out over the entire length of the structure s. Provided that no moving velocity discontinuities are present,

$$\int_s n(\ddot{u}_i - \ddot{u}_i^*)(\dot{u}_i - \dot{u}_i^*)\,\mathrm{d}s = \frac{d}{\mathrm{d}t}\int_s n(\dot{u}_i - \dot{u}_i^*)(\dot{u}_i - \dot{u}_i^*)\,\mathrm{d}s. \tag{2}$$

Further, for rigid–plastic materials,

$$\int_s (Q_j - Q_j^*)(\dot{q}_j - \dot{q}_j^*)\,\mathrm{d}s \geq 0. \tag{3}$$

Thus, if

$$\Delta(t) = \int_s \frac{n}{2}(\dot{u}_i - \dot{u}^*)(\dot{u}_i - \dot{u}_i^*)\,\mathrm{d}s \tag{4}$$

equation (1) implies that

$$\frac{\mathrm{d}\Delta}{\mathrm{d}t} \leq 0. \tag{5}$$

Δ is positive definite, and is zero only when the two responses are identical. It may therefore be interpreted as a measure of the difference between the two solutions, and (5) shows that the solutions converge on each other in this sense as time proceeds.

Suppose now that v_i represents a set of initial conditions for which the response $\dot{u}_i$ is not known. If the initial conditions can be changed to new values v_i^* for which the response $\dot{u}_i^*$ is known or can be simply determined, it can be expected that $\dot{u}_i^*$ will be a good approximation provided that $\Delta(0)$ is small in comparison with the energy in either solution. It must be emphasized that the approximating solution must be complete in all respects in order that (5) should hold.

Martin and Symonds used one degree of freedom (or mode) solutions as approximating solutions. Thus, the response $\dot{u}_i^*$ is taken to be of the form

$$\dot{u}_i^* = v^* \phi_i(s) T(t), \tag{6}$$

where v^* is an amplitude, $\phi_i(s)$ is a mode shape, and $T(t)$ is a dimensionless function of time such that $T(0) = 1$. The value of v^* is obtained by minimizing $\Delta(0)$ with respect to v^*. It can be shown that $T(t)$ will be a linear function of the form

$$T(t) = 1 - \frac{t}{t_f}. \tag{7}$$

The mode approximation can be used for the problem under consideration and may be illustrated by its application. The structure is a rectangular portal frame (Fig. 1) with

uniform physical properties. At time $t = 0$ a mass G strikes the structure at C with a transverse velocity v_0 (i.e. v_0 is normal to the plane ABCB'A') and remains attached to the structure. It is assumed that the material is rigid–perfectly plastic. The yield stress is independent of strain rate, and the effects of geometry changes are neglected. Shear and axial deformations are not considered, and the rotatory inertia of a structural element is assumed to be zero.

Since shear and axial forces are neglected, the yield surface may be represented as a curve in bending moment–torsion moment space. It will be assumed that this interaction is given by the rectangular figure in Fig. 2, with the limit torsion moment less than or equal

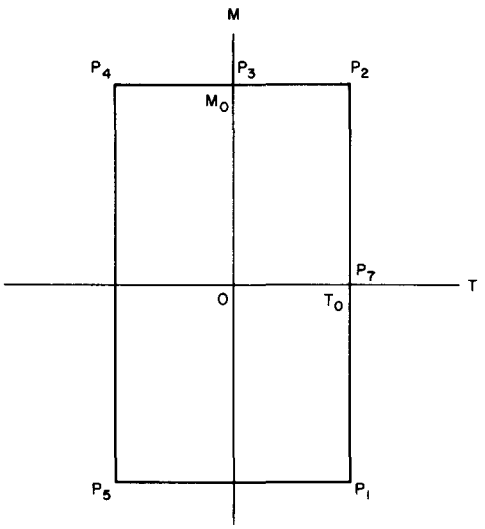

FIG. 2. Rectangular yield curve.

to the limit bending moment. The normality condition requires that along the lines of constant torsion moment (P_1P_2 and P_4P_5) the generalized strain rate vector is a twisting rate only. Similarly, along the lines of constant moment (P_4P_2 and P_5P_1) pure bending must occur. At the corner (P_1, P_2, P_4, P_5) the generalized strain rate vector, plotted at the corner, must be within the 90° fan formed by the outward normals to the two intersecting lines.

The actual yield curve for any symmetric section with the same yield stress in tension and compression will be symmetric about the M and T axes. Thus the rectangular interaction is an upper bound to all convex surfaces and will contain the actual yield surface.

The mode shape for this problem is shown in Fig. 3. This shape cannot be justified *a priori*; its acceptability is dependent on a check for yield violations in the structure. The initial velocity field is given by

$$\dot{u}^*(t = 0) = \frac{\mu}{2L}\dot{z}_0^* \qquad 0 < \mu < 2L \tag{8a}$$

$$\dot{u}^*(t = 0) = \dot{z}_0^* \qquad 0 < \lambda < L. \tag{8b}$$

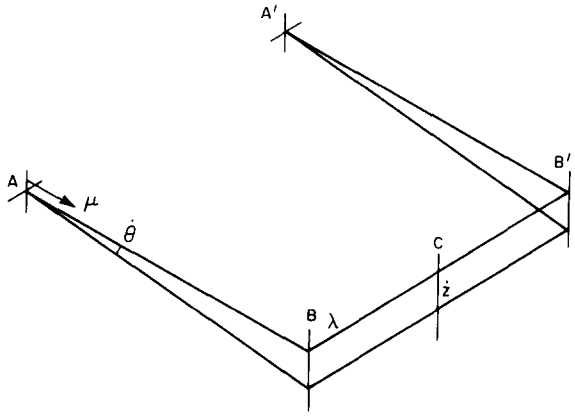

FIG. 3.

The actual velocity field is zero at all points except C, where the velocity is v_0. The appropriate form of equation (4) gives

$$\Delta(0) = \frac{G}{2}(v_0 - \dot{z}_0^*)^2 + \int_0^{2L} n\left(\frac{\mu \dot{z}_0^*}{2L}\right)^2 \mathrm{d}\mu + \int_0^L n(\dot{z}_0^*)^2 \,\mathrm{d}\lambda$$

$$= \frac{G}{2}(v_0 - \dot{z}_0^*)^2 + \tfrac{5}{3}nL(\dot{z}_0^*)^2. \tag{9}$$

The best initial value is found by minimizing $\Delta(0)$, and is given by

$$\dot{z}_0 = \frac{3}{3+10\gamma} \tag{10}$$

where

$$\dot{z}_0 = \frac{\dot{z}_0^*}{v_0}, \qquad \gamma = \frac{nL}{G} \text{ etc.}$$

The motion of the structure with the initial velocities defined by (8) and (9) will be derived in detail for later use, although it was shown [13] that in general the velocities will vary linearly with time and a simple expression can be written for the time at which motion ceases.

The hinges at A and A' etc. involve pure bending; it follows that the mode motion simply involves rotation of the structure about the line AA', with a restraining moment of $2M_0$. The equation of motion is thus obtained by setting the rate of change of angular momentum about AA' equal to $(-2M_0)$. Thus

$$\frac{d}{\mathrm{d}t}\left[2GL\dot{z}^* + 2\int_0^{2L} n\mu\left(\frac{\mu}{2L}\dot{z}^*\right)\mathrm{d}\mu + 4nL^2\dot{z}^*\right] = -2M_0. \tag{11}$$

Putting $t = M_0 t/GLv_0$, $\dot{z} = \dot{z}^*/v_0$, this reduces to

$$\dot{z} = \dot{z}_0 - \frac{3t}{(3+10\gamma)}. \tag{12}$$

The structure comes to rest when $t = t_f$, and

$$t_f = \left(1+\frac{10}{3}\gamma\right)\dot{z}_0. \tag{13}$$

The accelerations can be found from equations (12) and (8). The generalized stresses can now be found from equilibrium relations. It is found that the torsion moment T is zero, and the bending moment nowhere exceeds M_0. Hence the approximation is valid in the particular sense under discussion, and displacements may be found by integrating (12) and (8).

The final displaced shape predicted by the mode approximation will be proportional to the shape shown in Fig. 3. Although the magnitudes of the final displacements will represent a fairly good average displacement for the real problem, it is very clear that in this case the approximation is severely limited in that it predicts a constant displacement for the beam BCB'. It can be expected that deformation of the beam will take place, and that the relative deformations of B and C will depend on $\beta = T_0/M_0$.

The approximate technique may, however, be applied to more realistic initial conditions; it requires only that the solution to the modified initial conditions should be known. In the following section a more realistic approximation will be sought.

3. TWO DEGREE OF FREEDOM APPROXIMATIONS

Difficulty occurs in rigid–plastic analysis in finding approximate solutions to phases of the response in which travelling hinges occur. It seems reasonable, therefore, to seek in this case a fixed hinge solution which will allow relative deformation between B and C. To this end consider the initial velocity field shown in Fig. 4. This field has two parameters, $\dot{z}_0^*$ and $\dot{w}_0^*$, which must be determined. As in the mode solution the most rational choices of $\dot{z}_0^*$ and $\dot{w}_0^*$ which can be obtained from the initial data are those which minimize Δ^0, obtained by putting

$$\frac{\partial \Delta^0}{\partial \dot{z}_0^*} = \frac{\partial \Delta^0}{\partial \dot{w}_0^*} = 0. \tag{14}$$

For the real problem the initial velocity is zero everywhere except C, where the mass has velocity v_0. The approximate initial velocity field is

$$\begin{aligned} AB \quad & \dot{u}_0^* = \frac{\mu}{2L}\dot{w}_0^* \quad \text{for } 0 \le \mu \le 2L \\ BC \quad & \dot{u}_0^* = \left(1-\frac{\lambda}{L}\right)\dot{w}_0^* + \frac{\lambda}{L}\dot{z}_0^* \qquad 0 \le \lambda \le L. \end{aligned} \tag{15}$$

Hence

$$\begin{aligned} \Delta_0 &= \frac{G}{2}(v_0-\dot{z}_0^*)^2 + \int_0^{2L} w\left(\frac{\mu \dot{w}_0^*}{2L}\right)^2 \mathrm{d}\mu + \int_0^L n\left[\dot{w}_0^* + \frac{\lambda}{L}(\dot{z}_0^* - \dot{w}_0^*)\right]^2 \mathrm{d}\lambda \\ &= \frac{G}{2}(v_0-\dot{z}_0^*)^2 + \frac{nL}{3}[(\dot{z}_0^*)^2 + \dot{w}_0^*\dot{z}_0^* + 3(\dot{w}_0^*)^2]. \end{aligned} \tag{16}$$

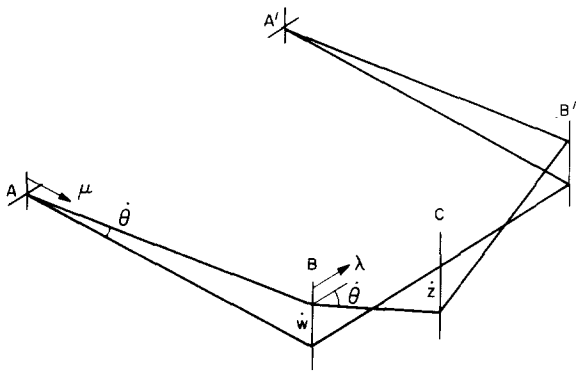

FIG. 4.

Differentiating and solving as in equation (14),

$$\dot{z}_0 = \frac{18}{18+11\lambda}$$

$$\dot{w}_0 = \frac{-3}{18+11\gamma} \tag{17}$$

where $\dot{z}_0 = \dot{z}_0^*/v_0$, $\dot{w}_0 = \dot{w}_0^*/v_0$.

Now that the initial velocity field of the approximating solution has been found, the analysis can proceed independently. It may be re-emphasized that the approximation involves only the determination of a suitable optimum initial velocity field. From this point a complete solution to the new problem must be found. It is this new solution which approximates the response to the initial velocity field.

Details of the solution will not be given, since the calculations are essentially straightforward and may be found by reference to Johnson [16]. Since the hinge positions are fixed, a technique related to Lagrange's principle was used to formulate the equations of motion. Suppose that the accelerations are $\ddot{u}(s)$, velocities $\dot{u}(s)$, the strain rates $\dot{q}_j(s)$ and the stresses $Q_j(s)$, where s is a variable measuring length along the beam. Let $\bar{v}(s)$ be a time independent velocity field with associated strain rates $\bar{q}(s)$. By the principle of virtual velocities

$$-\int n\ddot{u}\bar{v}\,\mathrm{d}s = \int_s Q_j\bar{q}_j\,\mathrm{d}s. \tag{18}$$

This equation may be integrated with respect to time to give

$$\int n\dot{u}_0(s)\bar{v}(s)\,\mathrm{d}s - \int n\dot{u}(s,t)\bar{v}(s)\,\mathrm{d}s = \int_{t_0}^{t_1}\mathrm{d}t\int_s Q_j\bar{q}_j\,\mathrm{d}s \tag{19}$$

where $\dot{u}_0$ denotes initial velocities. In this expression Q_j is not a function of time over certain phases of behavior because the hinges are fixed and because of the nature of the yield surface. In general, the behavior may be broken into a series of phases where expressions such as (19) can be applied. The initial conditions for an intermediate phase are simply the final velocities for the previous phase, and time is measured from the beginning

of the phase. Equation (19) is a necessary condition of equilibrium, and two such equations using two independent constant velocity field will provide the two relations necessary to find the two parameters which describe the velocity field. One such field is proportional to that shown in Fig. 3, and the other is given in Fig. 5. Proper account must be taken of the fact that the strain rates occur in discrete hinges, and the computation is still subject to a check that the yield condition is not violated.

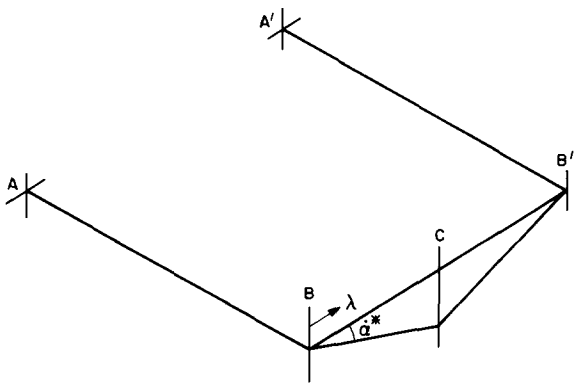

FIG. 5.

During the first phase of motion, starting with the conditions given in Fig. 4, the corner B moves downwards. The dimensionless velocities $\dot{w}$ at B and $\dot{z}$ at C (obtained by dividing real velocities by v_0) are given by

$$\begin{aligned} \dot{z} &= \dot{z}_0 - \left(\frac{45+42}{18+11}\right) t \\ \dot{w} &= \dot{w}_0 + \left(\frac{27+24\gamma+18\beta+18\beta\gamma}{\gamma(18+11\gamma)}\right) t. \end{aligned} \tag{20}$$

This phase ends at time t_1 when $\dot{w}$ becomes zero, since $\dot{w}_0$ (equation 17) is negative. The yield condition is not violated in this phase in the range $0 \leq \beta \leq 1$.

In the second phase $\dot{w}$ becomes positive, and the moment at A changes sign. The velocities are then given by

$$\begin{aligned} \dot{z} &= \dot{z}_1 - \frac{(39+42\beta)}{(18+11\gamma)}(t-t_1) \\ \dot{w} &= \frac{9+12\gamma+18\beta+18\beta\gamma}{\gamma(18+11\gamma)}(t-t_1) \end{aligned} \tag{21}$$

where $\dot{z}_1 = \dot{z}(t_1)$. This phase ends at $t = t_2$ when $\dot{w} = \dot{z}$, and the central hinge disappears. A check for yield violations shows that this behavior is valid only for

$$\beta \leq (4+\gamma)/(4+4\gamma). \tag{22}$$

Thereafter the behavior is given by the mode solution (equation 12) with $\dot{z}(t_2)$ substituted as the initial velocity.

When $\beta \geq (4+\gamma)/(4+4\gamma)$ the yield bending moment is exceeded at A during the second phase of this solution. It may be inferred that a hinge will form in AB, and the velocity field shown in Fig. 6 was assumed. In this case it is found that the hinge in AB remains stationary as the deformation continues, after jumping instantaneously from A at time t_1. This may be confirmed by a detailed analysis which permits the hinge to move [16], or by assuming that it is stationary and invoking the uniqueness proof [17] when a solution is found. The distance x is given by the expression

$$x = (3+2\gamma)+\frac{\sqrt{\{(17+24\gamma+8\gamma^2)+\beta(8+12\gamma+4\gamma^2)\}}}{2(1+\beta)(1+\gamma)}. \tag{23}$$

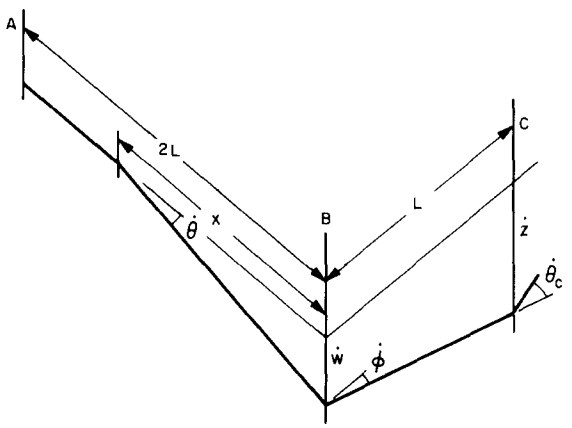

FIG. 6.

The velocities are given by

$$\dot{w} = \frac{6}{\gamma x^2}(t-t_1)$$

$$\dot{z} = \dot{z}_1 - \frac{6(1+x)}{x^2(1+\gamma)}(t-t_1). \tag{24}$$

This phase of motion ends when $\dot{z} = \dot{w}$ and the bar BCB' becomes rigid. A travelling hinge phase now takes place, with the hinge moving towards A. This presents no real problem, since it is similar to the cantilever beam problem solved in closed form by Parkes [6]. Since this may be considered as a standard solution in dynamic rigid–plastic theory, the results are quoted without development. $\bar{x}$ is a variable, denoting the hinge position as in Fig. 6.

$$\dot{z} = \dot{w} = \frac{(1+2\gamma+\gamma x)}{(1+2\gamma+\gamma\bar{x})}\dot{z}_2$$

$$t = t_2 + \frac{\gamma}{6}\bar{x}^2\dot{z} - \frac{\gamma}{6}x^2\dot{z}_2 \tag{25}$$

t_2, $\dot{z}_2$, x are respectively the time, velocity of the mass and hinge position at the end of the second phase.

This phase is completed in a short time, when the hinge reaches A. Thereafter the structure rotates about AA', as in the mode solution.

For comparative purposes an exact solution of the original problem (i.e. mass moving at velocity v_0) was attempted and is given in [16] for $\beta = 1.0$ and the range of parameters shown in the shaded area in Fig. 7. This solution is extremely complex, with the major difficulties occurring in the initial phases when hinges move away from the mass. After a short time the mechanisms used in the approximate solution are established, and the actual solution and the approximate solution thereafter are almost identical.

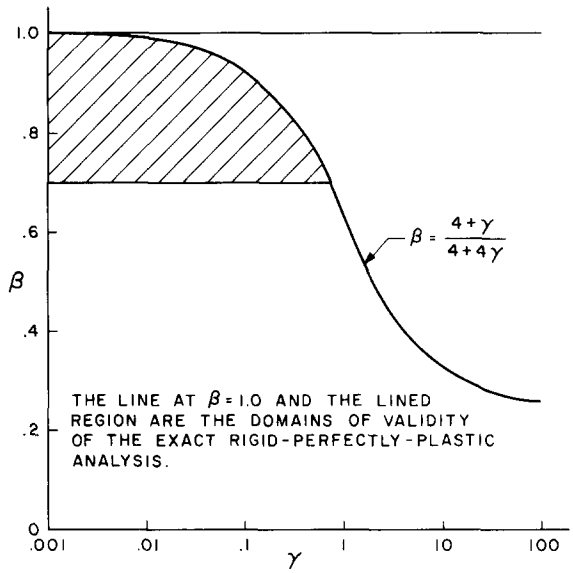

FIG. 7.

Figure 8 shows a comparison of the final displacement of the attached mass for various values of β and γ. It can be noted that in general the two degree of freedom approximation is a considerable improvement on the mode approximation, and that the further improvement obtained by an exact analysis is small. The ratio between the displacement of B, w, and the displacement of C, z, is given in Fig. 9. The mode approximation shows no variation with β and γ, and may seriously overestimate the displacement of the corner B. Typical velocity–time plots for the mass are shown in Fig. 10.

4. RIGID–VISCO-PLASTIC APPROXIMATE SOLUTION

Symonds [14] and Bodner [15] have used a one degree of freedom mode approximation as a basis for the construction of an approximate rigid–visco-plastic solution with some success in cantilever problems. A similar approximation may be found for the portal frame under discussion, based on the approximate rigid–plastic solution given in section 3. The rigid–visco-plastic approximation is motivated by the test results which are presented

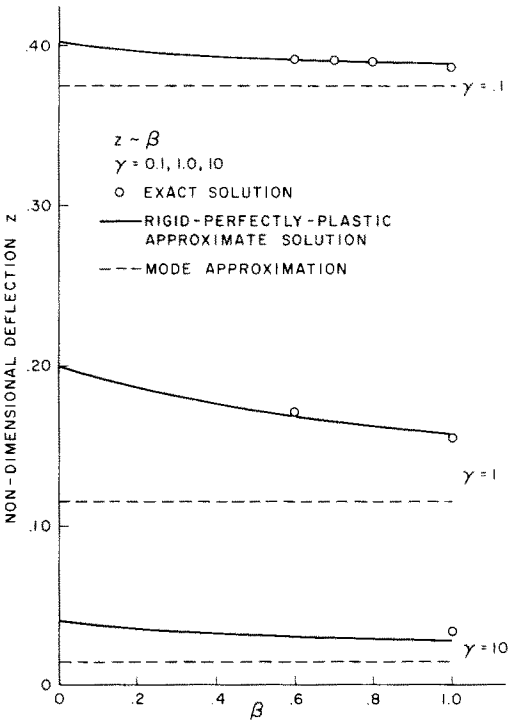
.40
.30
.20
.10
0
NON-DIMENSIONAL DEFLECTION z
z ~ β
γ = 0.1, 1.0, 10
EXACT SOLUTION
RIGID-PERFECTLY-PLASTIC APPROXIMATE SOLUTION
MODE APPROXIMATION
γ = .1
γ = 1
γ = 10
0
.2
.4
.6
.8
1.0
β

FIG. 8.

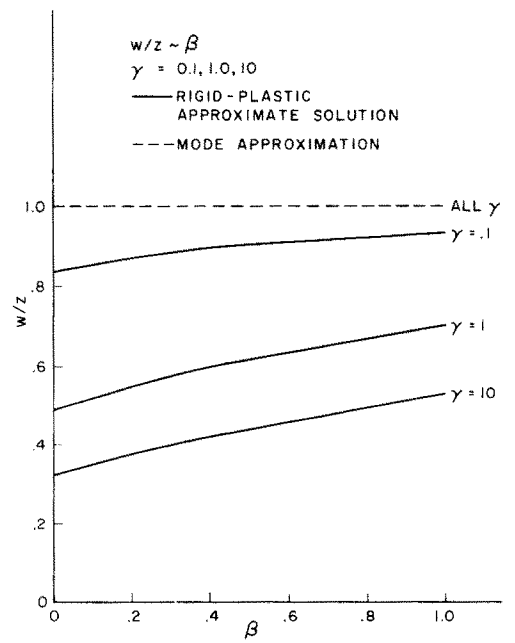
w/z ~ β
γ = 0.1, 1.0, 10
RIGID-PLASTIC APPROXIMATE SOLUTION
MODE APPROXIMATION
1.0
.8
.6
.4
.2
0
w/z
ALL γ
γ = .1
γ = 1
γ = 10
0
.2
.4
.6
.8
1.0
β

FIG. 9.

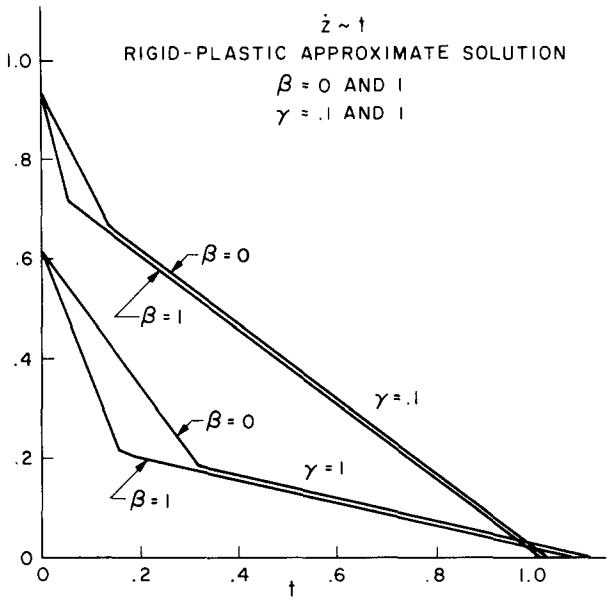

FIG. 10.

in the following section. In these experiments, on both steel and aluminum frames, discrepancies between the predictions of the elementary rigid–plastic theory and the test results are present which cannot be accounted for by strain hardening, geometry changes, or elastic effects.

The visco-plastic approximation is essentially a kinematic one. The values of the moments and torques at the hinges are replaced by elevated values obtained from an estimate of the curvature and twist rates at the hinges. As a result, the generalized stresses exceed the yield values over portions of the frame, but the strains in this region are not included in the analysis.

In one dimension, the relation between strain-rate $\dot{\varepsilon}$ and stress σ in a rigid–visco-plastic material will be taken to be of the form

$$\dot{\varepsilon} = \dot{\varepsilon}_0\left(\frac{\sigma}{\sigma_0} - 1\right)^p \quad \text{for } \sigma \geq \sigma_0$$
$$\dot{\varepsilon} = 0 \qquad\qquad \text{for } \sigma \leq \sigma_0 \tag{26}$$

where σ_0 is the static yield stress and $\dot{\varepsilon}_0$ and p are constants. A suitable generalization for complex stress states has been suggested by Perzyna [18].

$$\dot{\varepsilon}_{ij} = \gamma^0 \langle F^p \rangle \frac{\partial F}{\partial \sigma_{ij}} \tag{27}$$

where $\dot{\varepsilon}_{ij}$ and σ_{ij} are the strain-rate and stress tensors, and γ^0, p are constants

$$\langle F^p \rangle = F^p \text{ for } F \geq 0$$
$$\langle F^p \rangle = 0 \text{ for } F \leq 0$$
$$F = 0 \text{ is the initial yield surface.}$$

In this representation the yield surface expands isotropically as the magnitude of the strain-rate is increased.

Since no studies on sections subjected to combined bending and torsion in the visco-plastic range are known, it seems reasonable to base a relation on the isotropically expanding yield surface. For combined bending and torque, the lower bound on the initial yield surface (e.g. Hodge [19]) is given by

$$F = \left[\left(\frac{M}{M_0}\right)^2 + \left(\frac{T}{T_0}\right)^2\right]^{1/2} - 1 \tag{28}$$

Replacing $\dot{\varepsilon}_{ij}$ by the curvature and twist rates $\dot{K}$ and $\dot{\alpha}$, and σ_{ij} by the bending moment and torsion moment M and T, equation (27) then gives the following relations when only one generalized stress component acts on the section

$$\dot{K} = D\left\langle\left(\frac{M}{M_0} - 1\right)^p\right\rangle \quad \text{with } T = 0 \tag{29}$$

$$\dot{\alpha} = \frac{D}{\beta}\left\langle\left(\frac{T}{T_0} - 1\right)^p\right\rangle \quad \text{with } M = 0 \tag{30}$$

where $\beta = T_0/M_0$.

To be consistent with the rectangular yield surface used in the elementary rigid–plastic theory it will be assumed that equations (29) and (30) are valid for all M and T (in place of equation 28). The initial yield surface is then a rectangular shape defined by $M = \pm M_0$, $T = \pm T_0$.

In simple bending of a rectangular beam, it may be shown that the constant in equation (29) should be of the form

$$D = \frac{2\dot{\varepsilon}_0}{h}\left(\frac{2p+1}{2p}\right)^p \tag{31}$$

where h is the depth of the beam.

It is necessary to estimate the strain-rates in the hinges in order to use equations (29) and (30) to determine the elevated moments and torques. For this purpose a finite hinge length b is taken, and it is assumed that the strain-rates are uniform throughout the hinge. The rotation occurring in the hinge is the integral of the generalized strain along the hinge length, given in this case by strain times hinge length. All hinges (i.e. at A and C) are assumed to be of equal length, and thus

$$\begin{aligned} \dot{\alpha}_A &= \frac{\dot{\phi}}{b} \\ \dot{K}_A &= \frac{\dot{\theta}}{b} \\ \dot{K}_C &= \frac{\dot{\phi}}{b} \end{aligned} \tag{32}$$

where the subscripts refer to the hinges at A and C, and $\dot{\theta}$ and $\dot{\phi}$ are the rotation rates shown in Fig. 11. The rotation rates are related to the velocities $\dot{w}$ and $\dot{z}$ by the following equations.

$$\dot{\theta} = \frac{\dot{w}}{2L}$$
$$\dot{\phi} = \frac{\dot{z}-\dot{w}}{L} \tag{33}$$

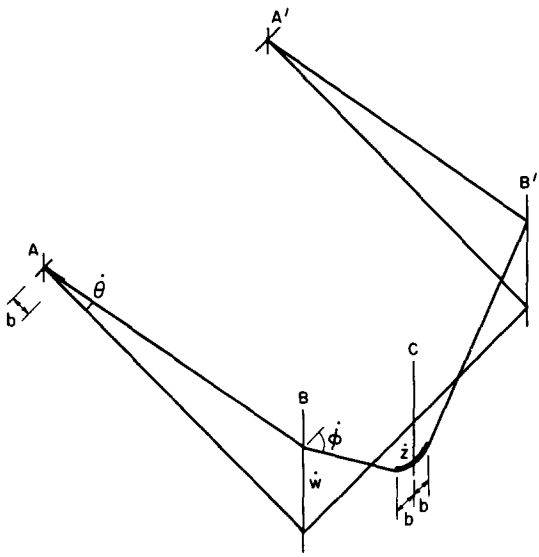

FIG. 11.

The hinge length b must also be specified. Examination of specimens in dynamic structural tests shows that the major part of the deformation is concentrated into a small length of beam comparable with the beam depth. Consequently, calculations will be carried out with $b = 2h$ and $b = 8h$. The two predictions obtained on this basis will provide a band which will cover most observations.

The analysis from this point follows closely that of the rigid–plastic approximate analysis. The experiments reported in the following section were designed to fall into the range

$$\beta \leq \frac{4+\gamma}{4+4\gamma} = R$$

and consequently the visco-plastic approximation will be developed for this case. It will be clear, however, that the approximation for $\beta > R$ will proceed in a similar manner.

The first phase velocity field is shown in Fig. 4, with the initial conditions given by

$$\dot{z}_0 = \frac{18}{18+11\gamma} \tag{34}$$

$$\dot{w}_0 = \frac{-3}{18+11\gamma}. \tag{35}$$

Three phases of behavior constitute the solution, as in the rigid–plastic approximation of the preceding section. The equations of motion are those of the rigid–plastic approximate analysis except with elevated moments M_A, M_C and T_A, and may be summarized in terms of the accelerations $\ddot{w}$ and $\ddot{z}$.

$$\text{First Phase } \ddot{w} = \frac{18(1+\gamma)\left[\frac{M_C}{M_0}+\beta\frac{T_A}{T_0}\right]+(9+6\gamma)\frac{M_A}{M_0}}{\gamma(18+11\gamma)} \tag{36}$$

$$\ddot{z} = -\left[\frac{42\left(\frac{M_C}{M_0}+\beta\frac{T_A}{T_0}\right)+\left|3\frac{M_A}{M_0}\right|}{(18+11\gamma)}\right] \tag{37}$$

with $|M_A/M_0|$ equal the absolute value of M_A/M_0.

$$\text{Second Phase } \ddot{w} = \frac{18(1+\gamma)\left(\frac{M_C}{M_0}+\beta\frac{T_A}{T_0}\right)-(9+6\gamma)\left(\frac{M_A}{M_0}\right)}{\gamma(18+11\gamma)} \tag{38}$$

$$\ddot{z} = -\left[\frac{42\left(\frac{M_C}{M_0}+\beta\frac{T_A}{T_0}\right)-3\frac{M_A}{M_0}}{(18+11\gamma)}\right] \tag{39}$$

$$\text{Third phase } \ddot{w} = \ddot{z} = -\frac{3\frac{M_A}{M_0}}{(3+10\gamma)} \tag{40}$$

The most comprehensive solution to these equations may be obtained by regarding M_A, M_C and T_A as functions of time, related to $\dot{w}$ and $\dot{z}$ through equations (33), (32), (30) and (29). The resulting differential equations are highly non-linear but in a form which can be readily solved numerically.

In solving the equations for the purpose of comparing theoretical predictions and experimental results, however, the approach of Perrone [10] and Bodner [15] will be followed. It will be assumed that the moments M_A, T_A and M_C are constant in each of the three phases. Thus equations (36) through (40) can be integrated directly for each phase (as in the rigid–plastic approximation). The constants of integration are determined from the initial conditions or the terminal values of the previous phase. In this approach the moment values M_A, T_A, M_C are found from the initial generalized strain-rates in each phase, and hence from the initial velocities in each phase. This approach is motivated by the nature of equations (29) and (30) when p is large (4 or 5 or larger). The moments will remain close to their initial values until the strain-rates vary significantly. When final displacements are compared, the effects of varying strain-rates are found to be very small.

5. EXPERIMENTAL STUDY

The purpose of the experimental study outlined below was to provide a preliminary check on the validity of the theoretical study present above. For this reason a comprehensive set of experiments was not planned. However, the four sets of experiments carried

out provide a reasonable variation in the non-dimensional parameters involved in the analysis (apart from $\beta = T_0/M_0$). The portal frames used in the experimental study were of square cross section for which, according to the von Mises yield condition, $\beta = 0{\cdot}77$. Two lengths L were chosen, approximately 2·5 and 5·0 in. A total of 16 experiments were performed, 8 with 6061-T6 aluminum alloy and 8 with 1021 mild steel.

The experimental apparatus is shown in the schematic diagram Fig. 12. An 8 in. wide flange beam was suspended as a simple pendulum. The specimen with its attached mass was clamped in the specimen holder, which was bolted securely onto the wide flange

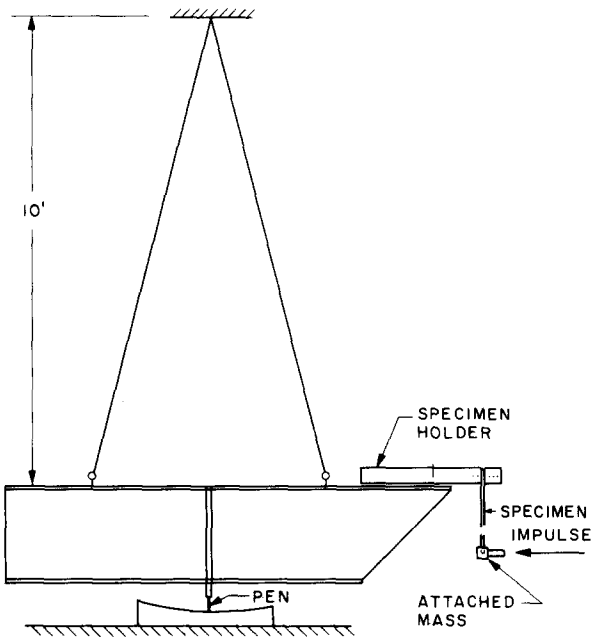

FIG. 12. Experimental apparatus.

beam. A pen for recording the amplitude of the oscillations was also attached to the beam.

The mass G of width $\frac{5}{8}$ in. was attached in such a manner that the $\frac{5}{8}$ in. length of beam (not included in the length L) onto which it was clamped would not deform during impact. The load was applied by the detonation of an electric blasting cap which was contained in a steel cylinder glued onto the attached mass. The steel cylinder disengaged from the attached mass immediately upon detonation of the blasting cap, i.e. the steel cylinder did not contribute to the attached mass. The natural period of vibration of the pendulum was much greater than that of the portal frame, which in turn, was much greater than the loading time. The load can thus be treated as an impulse. The impulse can be calculated since the distance from point of suspension to center of gravity, the suspended mass, and the amplitude of oscillation of the pendulum are known. To avoid extraneous vibrations the apparatus was designed so that the impulse would be applied at a point about the same level as the center of gravity of the suspended mass. To maintain this relationship, a spacer was inserted between the specimen holder and the wide flange beam when the longer specimens were tested.

The specimens were machined from sheet stock and were differently oriented in an effort to compensate for the effect of possible anisotropy due to rolling. Four ribbon test specimens were also machined from the sheet, two in the direction of rolling and two perpendicular to it. The aluminum alloy and steel ribbon specimens were subjected to simple tension tests and the stress–strain curves were found to exhibit slight strain hardening. The value of the yield stress σ_0 was based on the estimated strain due to bending in the portal frame specimens. The direction of rolling was found to affect the stress level about 10 per cent in the steel specimens and very little in the aluminum specimens. Typical stress–strain curves for the steel and aluminum ribbon specimens are shown in Figs. 13 and 14.

The final deformation of the attached mass and the corners of the frame were measured after detonation. The measurements, together with the complete data for each test, are given in Table 1.

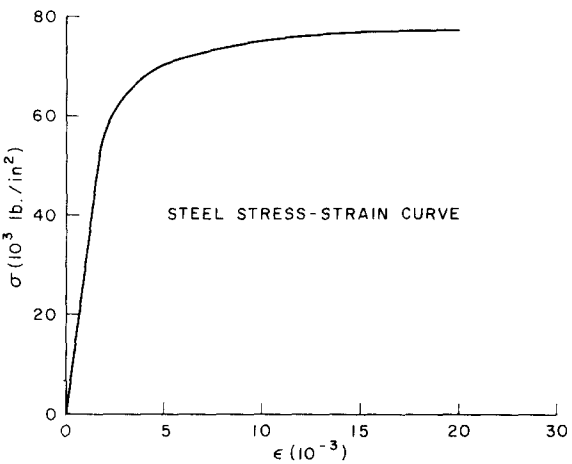

FIG. 13. Steel stress–strain curve.

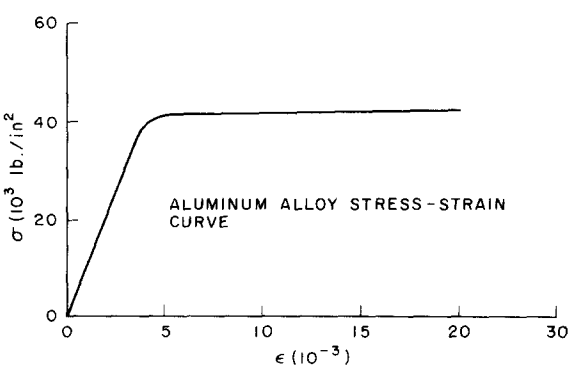

FIG. 14. Aluminum alloy stress–strain curve.

TABLE 1. EXPERIMENTAL RESULTS

A—Aluminum *S*—Steel

Test No.	γ	L in.	h in.	σ_0 lb/in^2	E^0 in. lb	v_0 in/sec	K^0 in. lb	Z_{exp} in.	W_{exp} in.	Z^* in. $b = 2h$	Z^* in. $b = 8h$	W^* in. $b = 2h$	W^* in. $b = 8h$
*A*1	0·1	2·5	0·25	46,100	17·3	550	60	0·41	0·36	0·39	0·41	0·352	0·396
*A*2	0·1	2·5	0·25	46,100	17·3	975	187·5	1·59	1·45	1·51	1·60	1·39	1·53
*A*3	0·1	2·5	0·25	46,100	17·3	810	130	1·06	0·96	1·01	1·07	0·932	1·03
*A*4	0·1	2·5	0·25	46,100	17·3	765	115·5	0·88	0·80	0·87	0·916	0·791	0·895
*A*5	0·1	2·5	0·25	46,100	17·3	1050	216	1·54	1·40	1·77	1·86	1·60	1·78
*A*6	1·0	5·3	0·40	42,200	79·2	2420	631	1·17	0·81	1·14	1·20	0·775	0·805
*A*7	1·0	5·3	0·40	42,200	79·2	2350	582	1·10	0·74	1·05	1·11	0·703	0·735
*A*8	1·0	5·3	0·40	42,200	79·2	2420	631	1·15	0·79	1·14	1·20	0·775	0·805
*S*1	0·1	2·5	0·25	90,000	22·7	435	107·5	0·295	0·275	0·274	0·306	0·258	0·305
*S*2	0·1	2·5	0·25	90,000	22·7	412	97·5	0·25	0·23	0·245	0·27	0·231	0·274
*S*3	0·1	2·5	0·25	90,000	22·7	417	99·6	0·285	0·265	0·25	0·278	0·235	0·281
*S*4	0·1	2·5	0·25	90,000	22·7	388	86·4	0·225	0·205	0·210	0·233	0·196	0·232
*S*5	1·0	5·0	0·35	75,000	62·2	1490	497	0·60	0·42	0·517	0·573	0·366	0·40
*S*6	1·0	5·0	0·35	75,000	62·2	1470	487	0·64	0·46	0·506	0·56	0·358	0·39
*S*7	1·0	5·0	0·35	75,000	62·2	1465	482	0·60	0·42	0·501	0·554	0·355	0·388
*S*8	1·0	5·0	0·35	75,000	62·2	1470	487	0·60	0·42	0·506	0·56	0·358	0·39

Z_{exp}, W_{exp} experimental results
Z^*, W^* predictions of approximate theory
E_0 elastic energy

Theoretical calculations were made using the approximate rigid–visco-plastic analysis given in the previous section. For mild steel the data of Manjoine [7] as expressed by Bodner and Symonds [8] was used for the dependence of yield stress on rate of strain.

$$\dot{\varepsilon} = 40\left(\frac{\sigma}{\sigma_0} - 1\right)^5 \tag{41}$$

For the 6061-T6 aluminum alloy, the relation was also taken from Bodner and Symonds' [8] work on cantilever beams

$$\dot{\varepsilon} = 6500\left(\frac{\sigma}{\sigma_0} - 1\right)^4. \tag{42}$$

The initial energy to be used in the theoretical calculations was modified slightly on the basis of the following argument. Consider a mass attached to a massless elastic–plastic spring, as shown in Fig. 15. Let the elastic slope be E, and the yield stress be σ_0. The mass has initial velocity v_0, corresponding to initial energy $K^0 = Gv_0^2/2$. The response of the system is shown in Fig. 30(b). The stress in the spring will increase from 0 to σ_0 (point P_1), and then remain constant until the strain reaches $\dot{\varepsilon}_{max}$, at P_2. At this point the work done will be equal to K^0. Thereafter a residual elastic vibration will take place in which the stress and strain vary between P_2 and P_3. If it is assumed that the residual vibration damps out symmetrically, the final strain will be given by ε_2. However, if the material is assumed

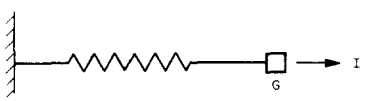

(a)

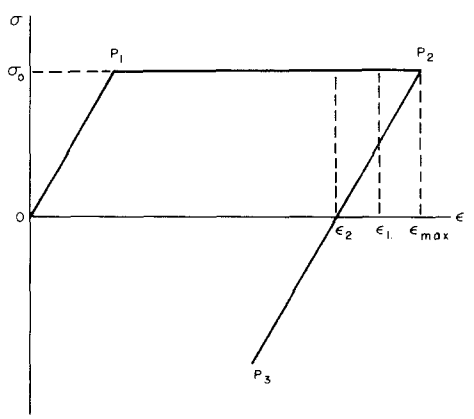

(b)

FIG. 15.

to be rigid–plastic, the final strain, given by

$$\varepsilon_1 = \frac{K^0}{\sigma_0} \tag{43}$$

will be the average of ε_2 and ε_{max}. In the form of equation (43), ε_2 is actually given by

$$\varepsilon_2 = \frac{K^0 - \sigma_0^2/2E}{\sigma_0} . \tag{44}$$

This implies that in order to obtain ε_2 by a rigid–plastic theory, the initial energy must be modified by subtracting the energy which can be stored elastically in the spring. If K^0 is very much larger than $\sigma_0^2/2E$, ε_1 and ε_2 will be very nearly the same. However, if the energy ratio is fairly small (as in some of the portal frames tested), the modification is significant. This procedure was followed in calculating the initial energy to be used in the analysis. The elastic energy was taken to be that stored in the frame when a point load (in the direction of the impulse) of a magnitude which would cause yield in the structure was placed at the point where the mass is attached.

A typical comparison of experimental results and theoretical calculations are given in Figs. 16 and 17. The displacement of the mass (z) and the displacement of the corner of the frame (w) are plotted for the 2·5 in. steel frames. Displacements are made dimensionless by dividing the predicted rigid–plastic displacement. Thus, in the theoretical results the effect of rate sensitivity is seen immediately. The results in the remainder of the tests

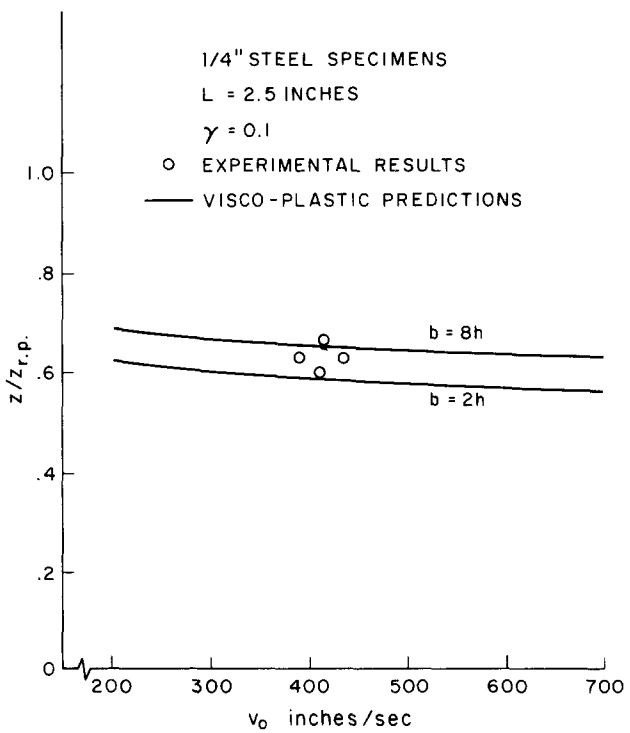

FIG. 16.

may be found in Table 1. In all except the 5 in. steel frames the experimental results lie within or very close to the band defined by hinge lengths of $2h$ and $8h$. In the 5 in. steel tests, the displacements are somewhat larger than predicted, but can nevertheless be considered to be in moderately good agreement with the theoretical results.

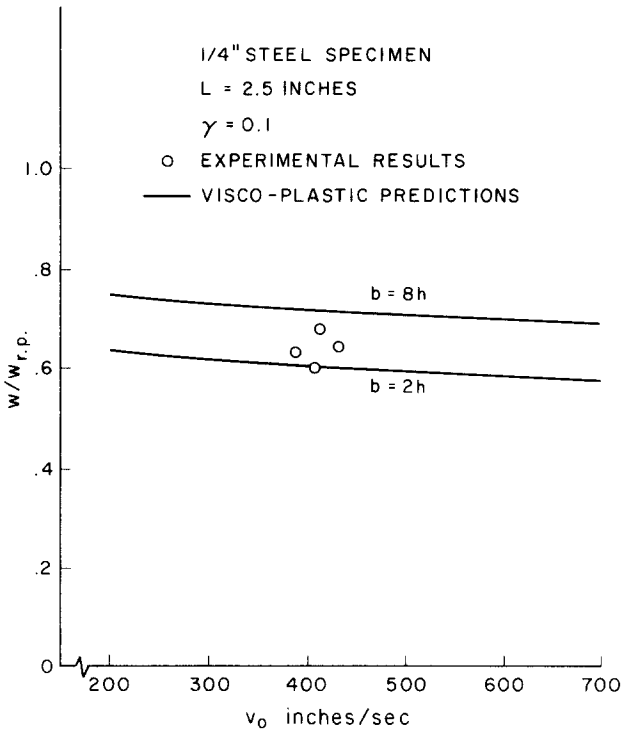

FIG. 17.

REFERENCES

[1] E. H. WITMER, H. A. BALMER, J. W. LEECH and T. H. H. PIAN, Large plastic deformations of beams, rings, plates and shells. *AIAA Jnl* **1**, 1848 (1963).
[2] E. H. LEE and P. S. SYMONDS, Large plastic deformations of beams under transverse impact. *J. appl. Mech.* **19**, 308 (1952).
[3] M. F. CONROY, Plastic–rigid analysis of long beams under transverse impact. *J. appl. Mech.* **19**, 465 (1952).
[4] H. G. HOPKINS and W. PRAGER, On the dynamics of plastic circular plates. *Z. angew. Math. Phys.* **5**, 317 (1954).
[5] P. S. SYMONDS, Simple solutions of impulsive loading problems and impact problems of plastic beams and plates, Tech. Rept. UERD-3 from Brown Univ. to the Norfolk Naval Shipyard under Contract N1895-1756A (April 1955).
[6] E. W. PARKES, The permanent deformation of a cantilever struck transversely at its tip. *Proc. R. Soc.* **A228**, 462 (1955).
[7] M. J. MANJOINE, Influence of rate of strain and temperature on yield stresses of mild steel. *J. appl. Mech.* **11**, A211 (1944).
[8] S. R. BODNER and P. S. SYMONDS, Experimental and theoretical investigation of the plastic deformation of cantilever beams subjected to impulsive loading. *J. appl. Mech.* **29**, 719 (1962).
[9] T. C. T. TING, The plastic deformation of a cantilever beam with strain rate sensitivity under impulsive loading. *J. appl. Mech.* **31**, 38 (1964).

[10] N. PERRONE, On a simplified method for solving impulsively loaded structures of rate sensitive materials. *J. appl. Mech.* **32**, 489 (1965).
[11] A. A. EZRA, The plastic response of a simply supported beam to an impact load at the center. *Proc. 3rd U.S. Natn. Congr. appl. Mech.* p. 513. ASME (1958).
[12] G. GANGOPADHYAY, Thesis presented to Brown University, in partial fulfillment of the requirements for the Master of Science degree.
[13] J. B. MARTIN and P. S. SYMONDS, Mode approximations for impulsively-loaded rigid–plastic structures. *J. Engng Mech. Div. Am. Soc. civ. Engrs* **92**, No. EM5, 43 (1966).
[14] P. S. SYMONDS, Viscoplastic behavior in response of structures to dynamic loading. *Proc. Colloq. on Behavior of Metals Under Dynamic Loading*, p. 106. ASME (1965).
[15] S. R. BODNER, Deformation of rate sensitive structures under impulsive loading. MML Report No. 7, Technion, Israel Institute of Technology (March 1967).
[16] G. L. JOHNSON, Ph.D. thesis, Division of Engineering, Brown University (1968).
[17] J. B. MARTIN, A note on the uniqueness of solutions for dynamically loaded rigid–plastic and rigid–viscoplastic continua. *J. appl. Mech.* **33**, 207 (1966).
[18] P. PERZYNA, The constitutive equations for rate-sensitive plastic materials. *Q. appl. Mech.* **20**, 321 (1963).
[19] P. G. HODGE, JR., *Plastic Analysis of Structures*, Chapter 9. McGraw-Hill (1959).

(*Received* 16 *November* 1967; *revised* 31 *October* 1968)

Абстракт—Приводится исследование действия неупругой реакции прямоугольной лормальной рамы, с присоединенной массой к центру ригеля, подверженной влиянию импульсной нагрузки, поперечной к плоскости рамы. Предлагается, что материал является жестко-пластическим, а взаимодействие между изгибом и кручением рассматривается на основе условия текучести представленного в виде прямоугольника. Обсуждаются, далее, отношение массы рамы к приложенной массе γ и отношение предельного крутящего момента к предельному моменту из гиба β, как переменные. Применяется простое решение двух степеней свободы для задачи при разных налльных условиях. Оно ислользуется для аппроксимации оригинальной задачи. Дается сравнение с точным жестко-пластическим решением для ограниченого диапазона величин β и γ. Проводились эксперименты на стальных и алюминиевых рамах. Импульсная нагрузка получена путем детонации взрцвчатых материалов, приложенных к присоединенным массам. Эксперименты указывают очевидность эффектов завимости напряжения текучести на скорость деформации. Если учитывается чувствительность скорости в решеню для двух степеней свободы приближенным способом, получается надлежащая корреляция между теорией и экспериментом.